Effect of Ether Electrolyte on the Electrochemical Performance of Cu₂S

Yingjie Zhang[1], Yongtai Li[2], Qiao Zhang[3], Chuan Shi[4], Xue Li[1,], Yiyong Zhang[1,*]*

[1] Faculty of Metallurgical and Energy Engineering, Kunming University of Science and Technology, Kunming 650093, China.
[2] Faculty of Materials Science and Engineering, Kunming University of Science and Technology, Kunming 650093, China.
[3] Faculty of Science, Kunming University of Science and Technology, Kunming 650093, China.
[4] College of Physics, Qingdao University, Qingdao, 266071, China..
[*]E-mail: 438616074@qq.com

With the widespread popularization of rechargeable portable devices, lithium-ion batteries have been researched in depth and have brought huge economic benefits. To improve the energy density and safety of lithium-ion batteries, research on new materials is urgent. Cu₂S has attracted the attention of researchers for its excellent physicochemical properties. It not only has an excellent reversibility of electrochemical lithium storage with high energy density but also has a low manufacturing cost. The electrolyte is responsible for transporting electrons and ions in the lithium battery. It is one of the important modules of the battery and has an important impact on the electrochemical performance of the battery. At present, there is very little research on the suitable electrolytes for Cu₂S. The effects of different types of ether electrolytes on the electrochemical performance of Cu₂S are studied in this paper. In addition, an activation process of the Cu₂S electrode material during the initial cycles is also studied.

1. INTRODUCTION

Research on rechargeable lithium-ion batteries began in the 1970s. The high energy density, Low accident rate, and long cycle life of lithium-ion batteries make it a market leader in energy storage equipment for portable electronic devices[1, 2]. At present, people have high requirements for the volume energy density and fast charge and discharge of lithium-ion batteries used in portable devices[3, 4]. Traditional lithium batteries use energy storage and release of lithium ions. However, structural limitations and low energy density make it impossible to achieve higher energy density

energy storage[5]. Electrode materials that rely on conversion reactions to achieve energy storage, such as metal sulfides, oxides, and fluorides, have received widespread attention because of their high specific capacities[6-8]. Metal sulfides have excellent physical and chemical properties and are widely used in solar cells, fast ion conductors, photocatalysis, semiconductor devices, sensitive components and other fields[9-15]. Cuprous sulfide material has excellent electrical conductivity (10^2 S·cm^{-1}), a high theoretical specific capacity (335 mAh·g^{-1}), a large energy density (1178 Wh·kg^{-1}), a flat discharge platform, and a low manufacturing cost[16-18]. It is a kind of anode material for lithium battery with great research significance. At present, many studies confirm that the charge-discharge process of Cu$_2$S follows the following conversion mechanism[19]:

$$2Li^+ + 2e^- + Cu_2S \rightarrow 2Cu + Li_2S \quad （1）$$
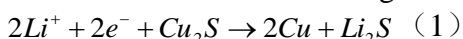
The main factors affecting the electrochemical performance of Li/Cu$_x$S battery systems are: (1) a volume change during the charge-discharge process; (2) decomposition or reaction of the electrolyte on the electrode; and (3) a capacity loss caused by dissolution of the active substance[20-22]. One of the main problems preventing Cu$_2$S electrode materials from being used in lithium-ion batteries is their poor cycling stability. During the charge-discharge process, Cu$_2$S will produce soluble lithium polysulfide[23, 24]. The polysulfide dissolved in the organic electrolyte may diffuse to the counter electrode and cause serious capacity loss. According to the current literature, the research on improving the electrochemical performance of Cu$_2$S anode materials is mainly focused on producing nanoscale structures and controlling the morphology. In many reports, after the production nanoscale material structure, the cycling performance has been improved to a certain extent. Han et al. prepared a Cu$_2$S/tubular mesoporous carbon composite with a high cycling stability and rate capability[25]. Cu$_2$S nanoparticles are highly dispersed throughout the tubular mesoporous carbon. In a 1 M LiTFSI DOL/DME (1:1, v/v) electrolyte, the composite material exhibits a high reversible capacity of 270 mAh·g^{-1} after 300 cycles at 0.2 C. Foley et al. obtained Cu$_2$S/C composite materials by vulcanizing and carbonizing copper-based organic framework materials[26]. Cu$_2$S nanoparticles are uniformly supported in the carbon framework. In a 1 M LiFP$_6$ EC/DEC (1:1 v/v) + 3% VC electrolyte, the material capacity is reduced by almost 70% after 100 cycles. Patil et al. synthesized Cu$_2$S-MoO$_3$ NC material by a one-step hydrothermal method, and the MoO$_3$ rods were surrounded by Cu$_2$S nanoparticles[27]. In a 1 M LiFP$_6$ EC/DEC (1:1 v/v) electrolyte, the specific capacity of the material was 1516 mAh·g^{-1} in the first cycle and 95 mAh·g^{-1} after 49 cycles. Therefore, the improvement of electrochemical performance not only relies on nanoscale materials and their special morphology but also finding suitable electrolytes should also be one of the research focuses.

The composition of the electrolyte solvent and the suitability of the active material is a research focus because it directly affects the electrochemical performance of the battery. Electrolyte solvents with different components have different solubilities toward polysulfide, and different degrees of decomposition or reaction will occur at the electrode. At present, little research has been done on the optimization of the solvent composition of liquid electrolytes, but it is generally believed that the use of ether-based solvents can improve the discharge capacity of lithium-sulfur batteries[28-30]. Thus, 1, 2-dimethoxyethane (DME) is a commonly used chain ether solvent. DME has a strong cation chelating ability and low viscosity (0.46 mPa·s), which can significantly improve the conductivity of the electrolyte, but it is extremely difficult to form an SEI film with the use of DME[29, 30]. The viscosity

of the electrolyte directly affects the discharge capacity. Low viscosities increase the utilization rate of the active substance but have a negative effect on capacity retention because it determines the solubility of the polysulfide[30]. 1, 3-Dioxolane (DOL) is a commonly used cyclic ether solvent that can improve the formation of a passivation layer on the lithium metal and has a high viscosity, thus improving the cycling performance of the batteries; however, DOL is prone to ring-opening polymerization[32]. In order to prevent lithium polysulfide from detaching from the electrode, it is common practice to add DOL to DME to reduce the ability of the electrolyte to dissolve lithium polysulfide. The combination of the two can not only obtain better electrical conductivity but also solve the problem that chain ethers are do not easily to form a film; at the same time the combination can obtain an appropriate viscosity, thereby improving battery performance[33].

Electrochemical properties of electrode materials using electrolytes with different components tend to vary widely. Therefore, it is questionable whether the proportion of solvents suitable for lithium-sulfur batteries is also suitable for Cu_2S anode materials, and no literature has been reported on it. To understand this question, this paper uses commercial cuprous sulfide as an electrode material and studies the difference in performance of Li/Cu_2S batteries in ether electrolytes with different ratios.

2. EXPERIMENT

Preparation of Cu_2S electrode: By a mass ratio of 70:15:15, the commercial Cu_2S material (Aladdin), acetylene black and PVDF were ground in a mortar and mixed evenly. A certain amount of N-methyl-2-pyrrolidone solvent (NMP) is added dropwise to the uniformly mixed powder. Grind for 30 minutes or more to make a powder slurry with an appropriate viscosity. The prepared powder paste was evenly coated on the aluminum foil collector by a scraper and dried at 60 °C for 12 h in a vacuum environment.

Physical characterization: The X-ray powder diffractometer (XRD, TESCAN, Mini Flex600) and scanning electron microscope (SEM, TESCAN, Vega3S) were used to analyze the phase structure and micromorphology of commercial Cu_2S.

Electrochemical test: For minimizing the effects of moisture and oxygen, the CR2016 button cell was assembled in an argon-filled glove box. Lithium sheet was used as the counter electrode, Celgard 2400 polypropylene film was used as the separator, 1 M LiTFSI DOL/DME = (9:1, 8:2, 7:3, 6:4, 5:5, 4:6, 3:7, 2:8, 1:9) v/v mixed solution as the electrolyte. The constant current charge-discharge test and the long-cycle test were performed by using the LAND test system at current density of 0.5 C and 2 C (1 C = 335 mAh·g^{-1}), and the voltage window was 1-3 V vs Li/Li$^+$.

3. RESULTS AND DISCUSSION

Fig. 1 is an XRD diffraction pattern of a commercial cuprous sulfide material. The results show that the purchased cuprous sulfide material contains three kinds of materials. The material is composed of cubic Cu_2S (JCPDS 03-1071) as the main phase and contains a small amount of CuS (JCPDS 06-

0464) and Cu (JCPDS 85-1326). Fig. 2 is an SEM image of a commercial Cu_2S material and an electrode surface. As shown in Fig. 2a, the morphology of the Cu_2S sample is irregular particles with a particle size between several hundred nanometers and 10 μm. Fig. 2b shows that the material and acetylene black are well mixed.
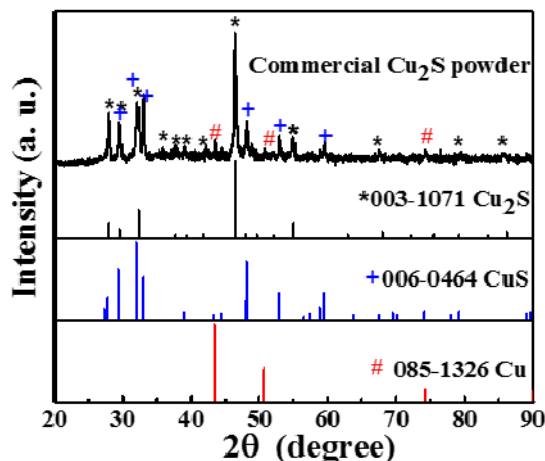
Figure 1. X-ray diffraction patterns of commercial Cu_2S powder.
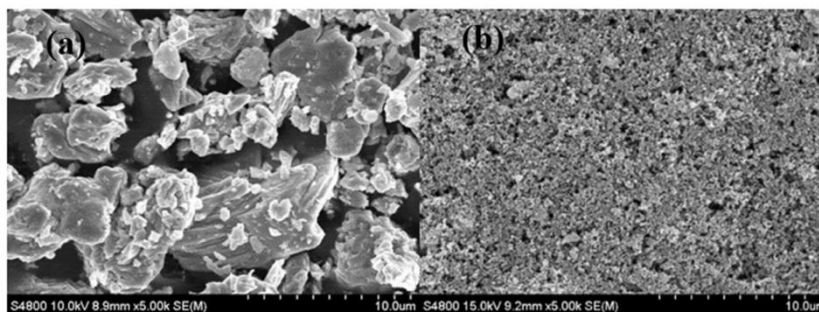
Figure 2. (a) SEM images of the commercial Cu_2S powder and (b) Cu_2S negative electrode.

Fig. 3 is the electrochemical performance of Li/Cu_2S batteries in different ether-based electrolytes. Fig. 3 (a) shows that in the electrolytes with different volume ratios of DOL and DME, the charge and discharge curves of the Cu_2S material in the first cycle are not very different. This shows that the composition difference does not affect the potential and length of the voltage plateau, and the first cycle capacity does not produce much difference. Fig. 3 (b) is the charge and discharge curve of the cuprous sulfide material after it is cycled to the 50th cycle under different component conditions. At this time, the differences in the electrochemical performance of the Cu_2S materials under different composition conditions gradually widen and the electrochemical curves of the three groups of DOL content greater than 70% show significant polarization and large capacity loss. Fig. 3 (c) is the cycle performance of Cu_2S material under the conditions of 9 kinds of electrolyte combinations. It can be seen that among the three components with a DOL content greater than 70%, the cycle performance of the battery is greatly affected, and the capacity begins to decay after 40

cycles. when the solvent component of the electrolyte is DOL/DME = 1:1, the cycle performance of the material is the best, which is the same as its optimal ratio in lithium-sulfur batteries.

When the content of the DOL component is more than 70%, the cycling performance of the battery will be greatly affected. The main reason is that DOL is relatively unstable and prone to ring-opening reactions. Therefore, if the proportion of DOL is too high, the stability of the electrolyte will be affected. In addition, an excessively high DOL ratio increases the viscosity of the electrolyte. Increasing the viscosity of the electrolyte will cause the conductivity to decrease, which will affect the performance of the battery. Therefore, in lithium-sulfur batteries, some researchers will avoid the use of DOL and instead use high-viscosity polyether solvent molecules [34].
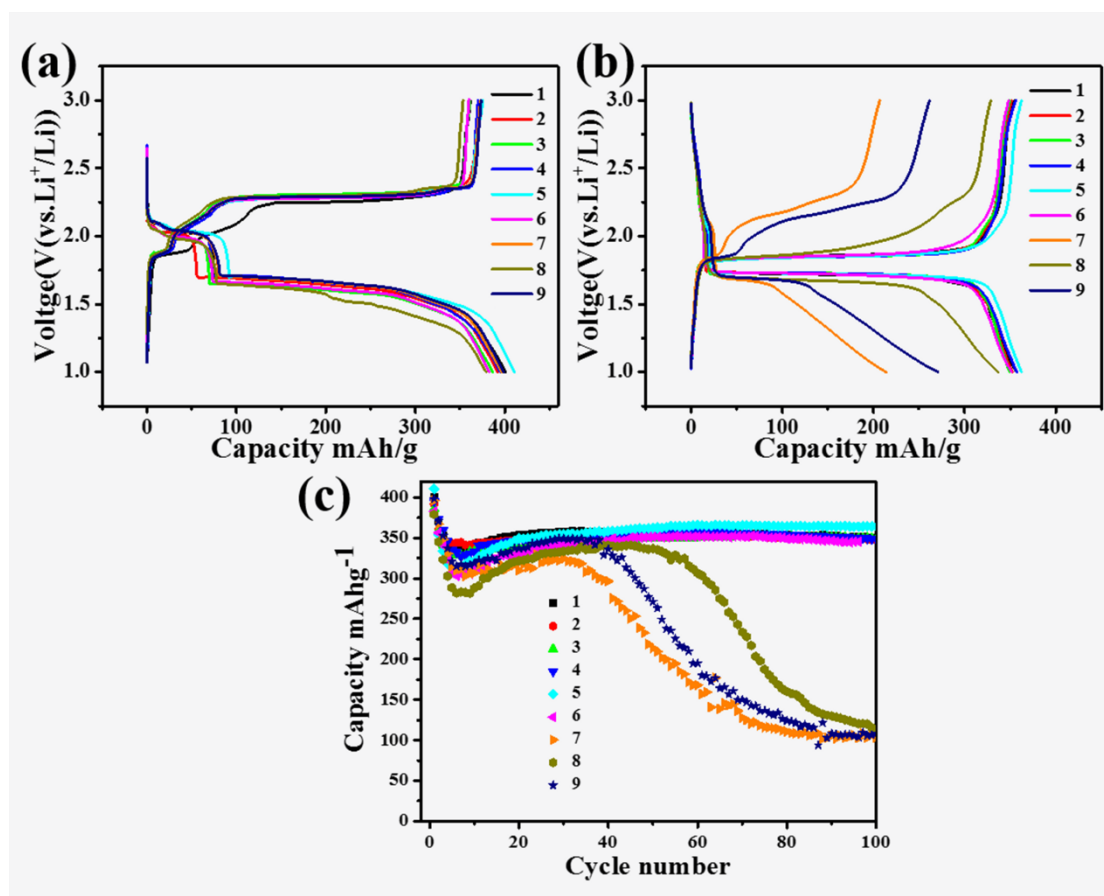
Figure 3. (a) Discharge and charge voltage profiles at the first cycle (0.5 C); (b) at the 50th cycle (0.5 C), and (c) the cycling performance of Li/Cu₂S cells in different electrolytes at a constant rate of 0.5 C. (Legend 1-9: DOL/DME = 1:9, 2:8, 3:7, 4:6, 5:5, 6:4, 7:3, 8:2, 9:1 v/v)

In order to more intuitively observe the effect of ether electrolytes with different DOL/DME ratios on the electrochemical performance of Cu_2S anode materials, the performance data of cuprous sulfide batteries are listed in Table 1. Table 1 shows that for the ether electrolytes with different DOL/DME ratios, the first-cycle discharge specific capacity of the Li/Cu_2S battery is kept at approximately 380 mAh·g^{-1}, and the first-cycle efficiency is approximately 93%. When the battery is cycled to the 100th cycle, the capacity retention rate between different proportions is greatly different.

When the DOL/DME ratio is 3:7 and 5:5, the capacity retention rate of the battery can reach above 90%. When the DOL/DME ratio is 6:4, the capacity retention rate drops to only 62.5%. when DOL/DME > 70%, the battery capacity will rapidly decay, and the capacity retention rate for 100 cycles is only 26.1% (7:3), 29.9% (8:2) and 27.0% (9:1). It can be known that the excessively high proportion of DOL in the electrolyte will seriously affect the electrochemical performance of Li/Cu_2S batteries.

Table 1. Comparision of the Li/Cu_2S cell performance in different electrolytes

DOL/DME	1:9	2:8	3:7	4:6	5:5	6:4	7:3	8:2	9:1
First cycle discharge capacity	400.9	392.0	386.6	394.9	382.9	382.6	396.2	379.2	398.6
First cycle charge capacity	374.7	372.9	361.2	370.2	356.5	360.2	367.2	353.5	373.6
First cycle Coulombic efficiency	0.935	0.951	0.934	0.937	0.931	0.941	0.926	0.932	0.937
100th cycle discharge capacity	350.3	347.6	349.1	348.3	346.0	239.3	103.3	113.5	107.8
100th cycle Coulombic efficiency	0.873	0.886	0.903	0.881	0.904	0.625	0.261	0.299	0.270

Fig. 4 (a) is the charge-discharge curve showing the first 20 cycles of the Cu_2S anode materials in the optimal component ether electrolyte (1 M LiTFSI DOL/DME = 1:1 v/v). The charge and discharge curve of the first circle shows that when the cuprous sulfide material is discharged for the first time, there will be two discharge plateaus of 2.05 V and 1.70 V and three charging plateaus of 1.85 V, 2.2 V and 2.3 V. The reason why the 2.05 V and 2.2 V plateaus appear in the charge and discharge curve is because the Cu_2S material contains a small amount of CuS. Because the theoretical specific capacity of CuS is 560 mAh·g^{-1}, the initial specific capacity of Li / Cu2S batteries appears to exceed the theoretical specific capacity. The charging and discharging mechanism of copper sulfide is divided into two steps:

$$CuS + Li \rightarrow 0.5Cu_2S + 0.5Li_2S \quad (2)$$
$$0.5Cu_2S + Li \rightarrow Cu + 0.5Li_2S \quad (3)$$
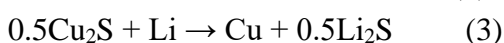
As the reaction progresses, CuS will gradually be converted to Cu_2S, and the corresponding high-potential platforms of 2.05 V and 2.2 V will gradually become shorter until they finally disappear. After 20 cycles, the Cu_2S material has only two stable plateaus, 1.7 V and 1.85 V. Some studies have defined these 20 cycles of charge and discharge cycles as "electrochemical activation processes"[35].
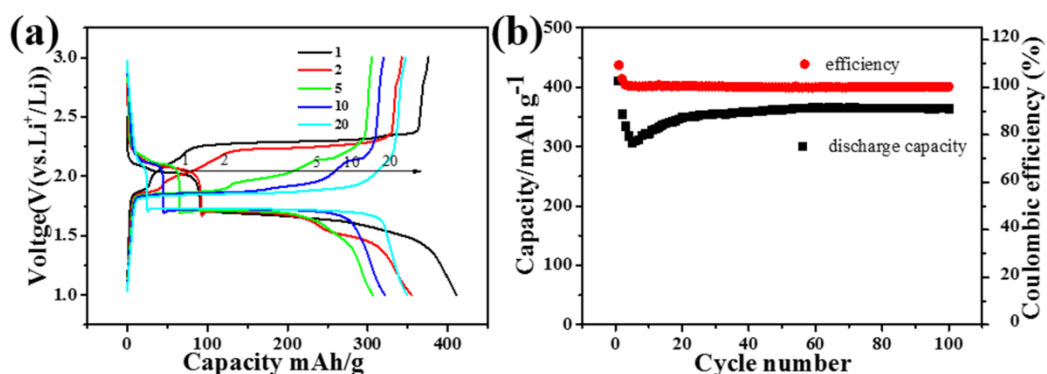
Figure 4. (a) Discharge and charge voltage profiles of the Li/Cu$_2$S cell in 1 M LiTFSI/ DOL/DME = 5:5 v/v for the first twenty cycles, (b) cycling performance and columbic efficiency of the Cu$_2$S electrode at a constant rate of 0.5 C.

Fig. 4 (b) shows the cycling performance of Cu$_2$S anode material in the optimal composition of the ether electrolyte when the current density is 0.5 C. Due to the previous activation process, the capacity retention rate in the first 20 cycles is unstable. After the material is activated, there is almost no attenuation in capacity, and the Coulombic efficiency remains close to 100%.

During the study of the suitability of the electrode material and the electrolyte, we find that under the electrolyte conditions of each component, the Cu$_2$S material has a high 2.3 V temporary potential plateau during the first two cycles. There is a large potential difference between this temporary potential plateau and the 1.85 V plateau after the activation is stable; thus, plateau will disappear rapidly and only exists in the first two charge and discharge cycles. Cui et al. reported that when lithium sulfide is directly used as an electrode, because lithium sulfide has a low conductivity and does not contain polysulfide ions in the electrolyte, it will cause a temporary potential plateau of 2.35 V during the first charge[36]. After being activated by charge and discharge cycle, a small amount of polysulfide ions gradually generates around the lithium sulfide, and the potential plateau located at 2.35 V will gradually disappear. Fig. 5 (a) is the charge and discharge curve of the Li/Cu$_2$S battery after activation in the optimal ether electrolyte component (1 M LiTFSI DOL/DME = 1:1 v/v). At this time, the battery only has plateaus at 1.7 V and 1.85 V. The battery that has been activated is disassembled in a fully charged state, replaced with a new electrolyte. Then, the battery's charge and discharge performance is retested. The results show that in the first two charging processes, the reassembled battery still has a 2.3 V charging plateau (as shown in Fig. 5 (b)), and the plateau disappears in the third charging cycle. This shows that in the cuprous sulfide battery, a temporary potential plateau caused by lithium sulfide also appears.

Fig. 6 is a battery performance diagram of the Cu$_2$S material after 5 cycles of 0.2 C low current activation, and then a long-term cycling test a rate of 2 C. When the small current cycle is performed, the battery capacity has a large attenuation. This is because the material contains a small amount of CuS impurities. Chung et al. pointed out that when a simple copper substance and lithium sulfide are converted into copper sulfide, it is largely irreversible, which will cause the capacity of the copper sulfide materials to decline[37]. During the 2 C charge and discharge cycling, there is also a gradual activation process of capacity because the small current activation time of 0.2 C is not enough.

However, the capacity of the Cu_2S material stabilizes at 310 mAh·g^{-1} after 20 cycles. After the battery is cycled to 500 cycles, the capacity is not reduced, and the Coulombic efficiency is maintained at 100%.
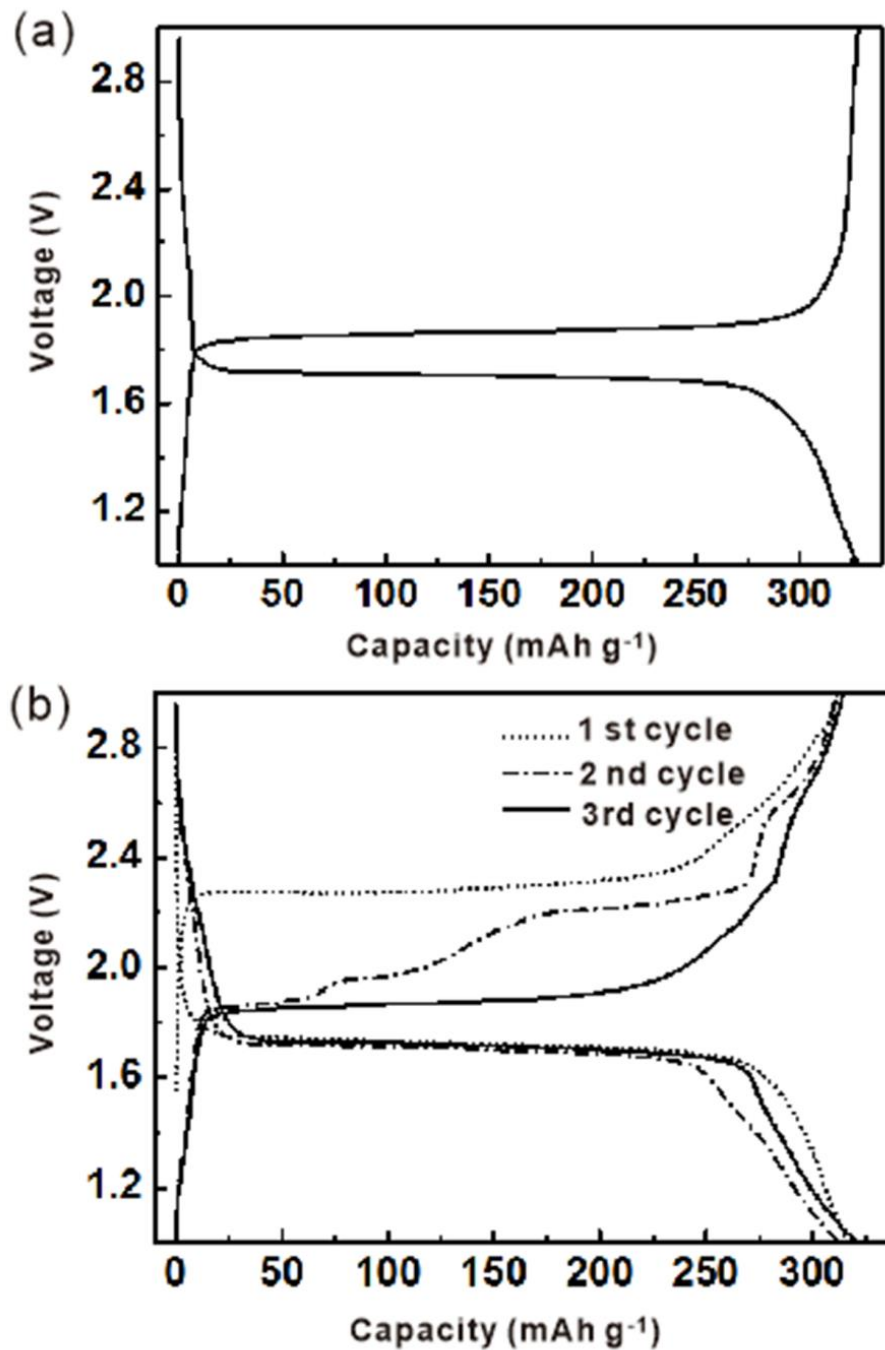
Figure 5. Voltage profiles of the Li/Cu_2S cells. (a) after the initial cycles and (b) reassembling the cell with fresh electrolyte.
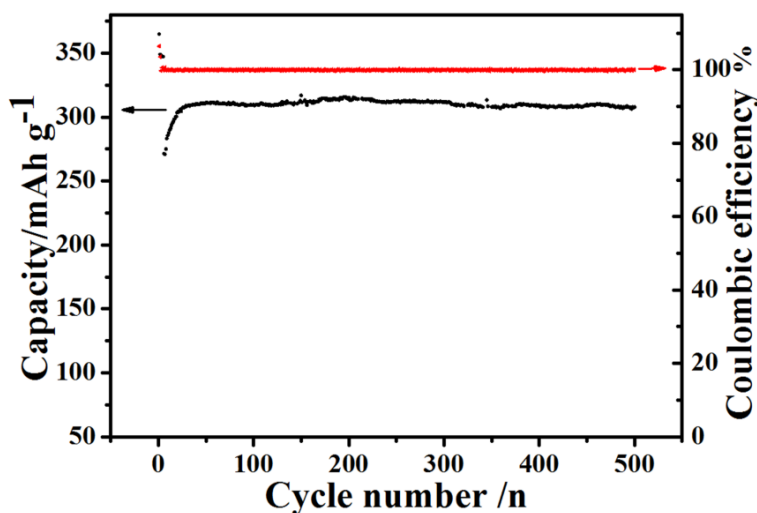
Figure 6. Cycling performance and Coulombic efficiency of the Cu_2S electrode in 1 M LiTFSI DOL/DME = 5:5 v/v electrolyte at a constant rate of 2 C.

4. CONCLUSIONS

This paper uses commercial cuprous sulfide as an electrode material to study the difference in performance of Li/Cu_2S batteries in ether electrolytes with different ratios. An X-ray diffraction comparison with commercial Cu_2S shows that the sample is mainly Cu_2S (JCPDS 003-1071), and also contains a small amount of CuS (JCPDS 006-0464) and Cu (JCPDS 085-1326). The Cu_2S anode materials has the best cycling performance in 1 M LiTFSI DOL/DME = 1:1 v/v ether electrolyte and the worst electrochemical performance in 1 M LiTFSI DOL/DME = 7:3 v/v ether electrolyte. Because Cu_2S material contains a small amount of CuS, the battery needs an activation process in the early cycle, and the battery's charge and discharge reaction is gradually stabilized during this activation process. The activation process is closely related to the presence of polysulfide ions in the battery system. After 20 cycles, the electrode material is completely converted to cuprous sulfide, and the charge-discharge curve becomes stable. Under the optimal ether electrolyte composition, the battery can achieve a long cycle life of 500 cycles under a large current density of 2 C, the capacity is stable at about 310 mAh·g^{-1}, and the Coulombic efficiency is 100%.

References

1. A. Débart, L. Dupont, R. Patrice and J.-M. Tarascon, *Solid State Sci.*, 8(2006)640-651.
2. C. Y. Nan, Z. Lin, H. G. Liao, M. K. Song, Y. D. Li and E. J. Cairns, *J. Am. Chem. Soc.*, 136(2014)4659-4663.
3. D. C. Lin, Y. Y. Liu and Y. Cui, *Nat. Nanotechnol.*, 12(2017)194.
4. L. Chen, Y. Z. Liu, M. Ashuri, C. H. Liu and L. L. Shaw, *J. Mater. Chem*. A, 2(2014)18026-18032.
5. G. Kalimuldina and I. Taniguchi, *J. Mater. Chem*. A, 5(2017)6937-6946.
6. H. Li, Y. H. Wang, J. X. Huang, Y. Y. Zhang and J. B. Zhao, *Electrochim. Acta,* 225(2017)443-451.
7. J. Ko and Y. S. Yoon, *Ceram. Int*., 45(2019)30-49.

8. S. H. Yu, S. H. Lee, D. J. Lee, Y. E. Sung and T. Hyeon, *Small,* 12(2016)2146-2172.
9. F. Ghribi, A. Alyamani, Z. B. Ayadi, K. Djessas and L. E. Mir, *Energy Procedia*, 84(2015)197-203.
10. A. Heerwig, R Merkle, J. Maier and M. Ruck, *J. Solid State Chem*., 184(2011)191-198.
11. F. Li, J. F. Wu, Q. H. Qin, Z. Li and X. T. Huang, *Powder Technol*., 198(2010)267-274.
12. A. Amlouk, K. Boubaker and M. Amlouk, *Vacuum*, 85(2010)60-64.
13. P. F. Qiu, Y. Q. Zhu, Y. T. Qin, X. Shi and L. D. Chen, *APL Mater.,* 4(2016)104805.
14. H. S. Song, A. P. Tang, G. R. Xu, L. H. Liu, M. J. Yin and Y. J. Pan, Int. J. Electrochem. Sci., 13(2018)4720-4730.
15. H. S. Song, A. P. Tang, G. R. Xu, L. H. Liu, Y. J. Pan and M. J. Yin. Int. J. Electrochem. Sci., 13(2018)6708-6716.
16. Q. W. Chen, M. M. Ren, H. Xu, W. L. Liu, J. P. Hei, L. W. Su and L. Z. Wang, *ChemElectroChem*, 5(2018)2135-2141.
17. C. H. Lai, K. W. Huang, J. H. Cheng, C. Y. Lee, B. J. Hwang and L. J. Chen, *J. Mater. Chem*., 20(2010)6638-6645.
18. S. R. Kadam, R. S. Kalubarme, S. P. Deshmukh, R. P. Panmand, U. V. Kawade, M. V. Kulkarni, S. S. Deo, S. W. Gosavi and B. B. Kale, *ChemistrySelect*, 3(2018)11020-11026.
19. G. Kalimuldina and I. Taniguchi, *Electrochim. Acta*, 224(2017)329-336.
20. G. Eichinger and H. P. Fritz, *J. Electroanal. Chem. Interfacial Electrochem*., 58(1975)357-367.
21. F. W. Dampier, *J. Electrochem. Soc*., 128(1981)2501-2506.
22. F. Bonino, M. Lazzari, B. Rivolta and B. Scrosati, *J. Electrochem. Soc*., 131(1984)1498-1502.
23. R. Cai, J. Chen, J. X. Zhu, C. Xu, W. Y. Zhang, C. M. Zhang, W. H. Shi, H. T. Tan, D. Yang and H. H. Hng, *J. Phys. Chem*. C, 116(2012)12468-12474.
24. C. Xu, Y. Zeng, X. H. Rui, N. Xiao, J. X. Zhu, W. Y. Zhang, J. Chen, W. L. Liu, H. T. Tan and H. H. Hng, *Acs Nano*, 6(2012)4713-4721.
25. F. Han, W. C. Li, D. Li and A. H. Lu, *ChemElectroChem*, 1(2014)733-740.
26. S. Foley, H. Geaney, G. Bree, K. Stokes, S. Connolly, M. J. Zaworotko and K. M. Ryan, *Adv. Funct. Mater.*, 28(2018)1800587.
27. S. B. Patil, B. Kishore, K. Manjunath, V. Reddy and G. Nagaraju, *Int. J. Hydrogen Energy*, 43(2018)4003-4014.
28. D. R. Chang, S. H. Lee, S. W. Kim and H. T. Kim, *J. Power Sources*, 112(2002)452-460.
29. J. W. Choi, G. Cheruvally, D. S. Kim, J. H. Ahn, K. W. Kim and H. J. Ahn, *J. Power Sources*, 183(2008)441-445.
30. C. Barchasz, J. C. Leprêtre, S. Patoux and F. Alloin, *Electrochim. Acta*, 89(2013)737-743.
31. J. W. Choi, J. K. Kim, G. Cheruvally, J. H. Ahn, H. J. Ahn and K. W. Kim, *Electrochim. Acta*, 52(2007)2075-2082.
32. H. S. Kim and C. S. Jeong, *Bull. Korean Chem. Soc*., 32(2011)3682-3686.
33. W. K. Wang, Y. Wang, Y. Q. Huang, C. J. Huang, Z. B. Yu, H. Zhang, A. B. Wang and K. G. Yuan, *J. Appl. Electrochem*., 40(2010)321-325.
34. X. Ji and L. F. Nazar, *J. Mater. Chem*., 20(2010)9821-9826.
35. Y. J. Li, X. C. Sun, Z. J. Cheng, X. Xu, J. Pan, X. F. Yang, F. Tian, Y. L. Li, J. Yang and Y. T. Qian, *Energy Storage Mater*., 22(2019)275-283.
36. Y. Yang, G. Y. Zheng, S. Misra, J. Nelson, M. F. Toney and Y. Cui, *J. Am. Chem. Soc*., 134(2012)15387-15394.
37. J. S. Chung and H. J. Sohn, *J. Power Sources*, 108(2002)226-231.